

# Vibration damping capability of electrical discharge machined surfaces: Characteristics, mechanism and application

Felipe Coelho, Philip Koshy \*

*Department of Mechanical Engineering, McMaster University, Hamilton, Canada*

---

## Abstract

This research explored frictional energy dissipation aspects of electrical discharge machined (EDM) surfaces in the context of passive vibration damping. The effect of discharge current and duration was investigated to characterise the damping capability of these surfaces, and to understand the underlying mechanisms. Topographic analyses indicated the damping ratio to be maximised through an interaction between positive skewness and elevated kurtosis of surface height, which facilitates recurrent microslip and plastic deformation at asperity contact edges. This renders EDM textures to be uniquely disposed to vibration control, as demonstrated by their efficacy in enhancing the dynamic performance of a grooving tool.

*Key words:* Chatter, Electrical discharge machining (EDM), Frictional energy dissipation, Microslip, Passive vibration damping

---

Int. J. Mach. Tools & Manuf. 177 (2022) 103888

## 1 Introduction

Self-excited vibration, known as chatter, limits material removal rate, surface quality and accuracy in cutting, and could cause structural damage to the machining system. Passive damping avenues to mitigating chatter have largely entailed tuned mass dampers and high-damping materials; frictional energy dissipation at contact interfaces is a simple and elegant approach to damping, on which the literature is but relatively scant [1].

---

\* Corresponding author

*Email address:* `koshy@mcmaster.ca` (Philip Koshy).

Ziegert et al. [2] assembled a flexible cylindrical insert with multiple fingers into a hollow end milling tool, such that spindle rotation-induced centrifugal force and cutting force-induced tool bending combine to cause sliding of said fingers against the tool body to dissipate energy. This yielded a 53% increase in the stability-limited cut depth. Likewise, Hayati et al. [3] drilled holes parallel to the axis of a boring bar into which longitudinal pins were press fit. Vibration of this composite tool during the boring process develops friction between the shank and the embedded pins, which resulted in a 35% increase in the damping ratio  $\zeta$ .

Damping in a structure comprising an assembly is typically an order of magnitude higher than that of its monolithic equivalent, which attests to the significance of damping at joint interfaces relative to material damping. The manufacturing process used to generate the surfaces constituting the joint, in conjunction with their roughness and lay direction, exert a complex influence on the extent of transverse frictional damping [4]. Along these lines, the present research investigated the damping potential of interfaces generated using sink electrical discharge machining (EDM).

The unconventional application of EDM in vibration damping was motivated in part by the work of Medina et al. [5]. Their numerical simulations predicted energy dissipation in laterally reciprocating rough contacts to increase with the kurtosis of surface height, for surfaces with a positively skewed height distribution (Fig. 1a). An examination of the skewness-kurtosis envelopes of typical machining processes [6] in this regard indicates EDM to be virtually the only process capable of generating isotropic surfaces with a positive skewness (Fig. 1b). A positive skewness denotes a height distribution that tails off

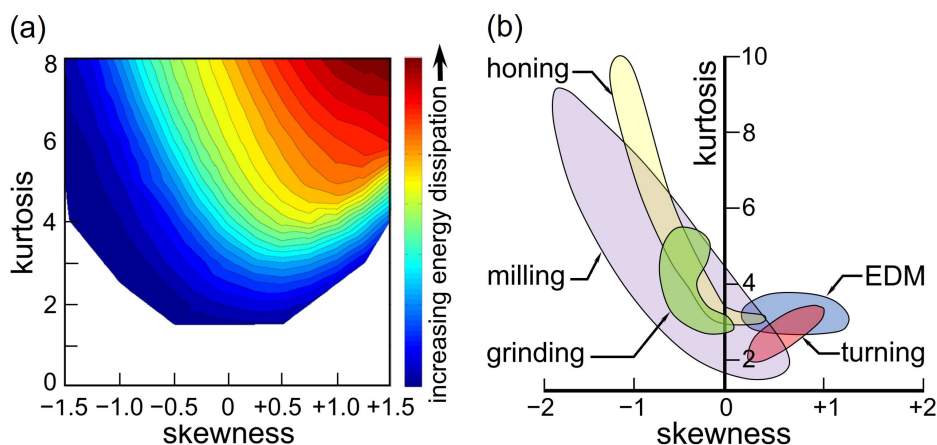


Fig. 1. (a) Effect of surface topography on energy dissipation; adapted from [5], and (b) skewness-kurtosis profiles of machining processes; after [6].

asymmetrically towards higher values.

This innovation is interesting also from the viewpoint of EDM, considering that its relatively poor material removal rate is of no consequence in such texturing applications, which involve an insignificant removal volume. Surface integrity issues that could arise in EDM under high discharge energy are as well of little detriment. EDM process parameters viz., the discharge current  $i_e$  and the discharge duration  $t_e$ , may further be readily manipulated to tailor the crater geometry towards maximising the damping capacity of the surface.

Beards and Neroutsopoulos [7] reported on  $\zeta$  of three EDM-ed mild steel surfaces of roughness 2.5, 4.2 and 5.4  $\mu\text{m}$   $Ra$  obtained by varying  $i_e$ . Their tests involved a forcing frequency of 132 Hz and an amplitude of 0.13 mm. Relative to a ground surface of 0.15  $\mu\text{m}$   $Ra$  roughness that yielded a  $\zeta$  of 1%, the least rough from among the three EDM surfaces corresponded to the best  $\zeta$  of 1.8%. On sustained loading,  $\zeta$  increased to 2.3% over  $10^7$  cycles due to accumulation of wear debris in the interface, during which course there was only a 10% drop in the dynamic stiffness of the joint. Intriguingly, they found the EDM-ed joints to refer to a four-fold lower fretting wear relative to ground counterparts even in the worst case, despite the intrinsic link between frictional damping and fretting corrosion; the joints as well corresponded to negligible loss of static stiffness.

A literature search returned just [7] above, published over 40 years ago, presenting rather elementary aspects of frictional damping related to EDM surfaces. Hayati et al. [3] did utilise EDM to drill holes in their anti-vibration boring bar, conceivably due to close tolerance ( $\sim 10 \mu\text{m}$ ) and high aspect ratio ( $\sim 45$ ) requirements, apparently unaware of the inadvertent role of the EDM texture in promoting frictional damping. In this context, the present work focused on the characteristics, mechanism, and application of damping from EDM-ed interfaces.

## 2 Experimental

The experimental work comprised two phases. In the first phase, vibration damping characteristics of EDM surfaces were investigated in a simple cantilever setup. Damping inserts accommodated within the test assembly were textured in a sink-EDM machine tool using a hydrocarbon dielectric fluid. Texturing involved positively polarised copper tools, an average gap voltage of 100 V and a duty factor of 0.5. Modal impact tests were conducted to obtain

the frequency response function (FRF), from which  $\zeta$  was estimated for the critical mode of vibration using the half-power method.

The discharge parameters  $i_e$  and  $t_e$  were varied systematically to quantify their influence on  $\zeta$  with a view to maximising damping performance. The generated surfaces were characterised in terms of roughness indices to detect possible correlations with  $\zeta$ . Some surfaces were selectively chosen for a visual topographic examination using a confocal microscope to decipher the mechanism of damping. Recognition of the mechanism in turn led to a hypothesis to further enhance damping, which was also verified and quantified. The second phase of experiments sought to demonstrate the application potential of the knowledge gained from the first, in enhancing the dynamic performance of an external grooving tool that is inherently prone to chatter.

### 3 Results & Discussion

#### 3.1 Characteristics and Mechanism

Figure 2a shows the experimental setup used in the first phase of experiments that comprised a 300 mm long cold-rolled AISI 1020 steel cantilever of section  $20 \times 50$  mm<sup>2</sup>. Damping inserts of length 85 mm and thickness 5 mm made from 6061 aluminum were sandwiched between the beam and steel loading plates at the top and bottom. Aluminum was chosen owing to its exceptional machinability in EDM, and its superior damping capacity derived partly from its relatively low Young's modulus [8]. The assembly involved two M8 bolts fastened to a torque of 11.3 Nm, which related to an estimated nominal normal pressure of  $\sim 4$  MPa at the insert interfaces, which is on the same order as that in [7]. Modal tap tests involved a maximum impact force of  $165 \pm 15$  N in the X-direction as shown in Fig. 2a.

Preliminary experiments assessed the performance of EDM-textured ( $i_e$  39 A,  $t_e$  112  $\mu$ s) damping inserts relative to extruded inserts of roughness  $1.8 \mu\text{m } Ra$  and the baseline case of no damping inserts, and the effect of insert location: top, bottom, and both. The red lines in Fig. 2a denote the textured side of the damping inserts facing the steel beam. Figure 2b presents  $\zeta$  extracted from the dominant first mode of vibration, wherein the error bars denote 95% confidence limits (as is the case throughout this paper). It is clearly evident that the insert is of little influence relative to the baseline when positioned at the top, be it extruded or textured; when positioned at the bottom, however,

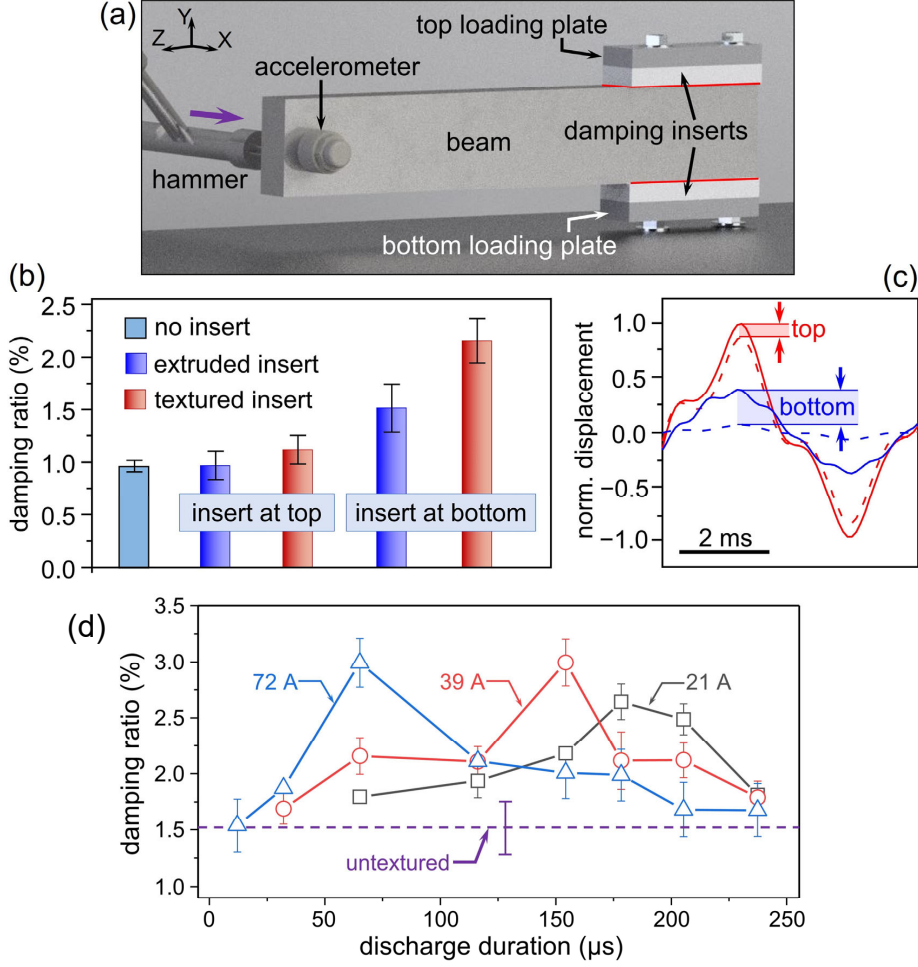


Fig. 2. (a) Experimental setup, (b) comparison of damping ratios, (c) temporal progression of normalised displacement between the insert (dashed line) and beam (solid line) across the interfaces, and (d) effect of discharge duration and current on the damping ratio.

the textured insert offers enhanced damping over that of the extruded one, and corresponds to more than a 100% increase in  $\zeta$  over the baseline. Inserts located at both the top and bottom did not offer any additional benefit, and hence further experiments employed only a single insert positioned below the beam.

To understand the effect of insert position, a finite element model was built to simulate the transient response of the beam during a tap test. The bottom of both bolts and the edges of the bolt holes on the underside of the bottom insert were constrained. The interfaces between the inserts and the beam were configured to allow slipping but no separation or penetration, with a coefficient of friction of 0.61 for the aluminum-steel pair. The model was validated

in terms of natural frequencies. The predicted frequencies for the three modes were 175, 540 and 1370 Hz, and the respective measured values were 188, 590 and 1391 Hz, which refers to a maximum deviation of just  $\sim 10\%$ . Probing the model for displacements of interest enabled the insight that the comparatively higher damping from the insert located at the bottom to be due to the larger relative displacement between the steel beam and the insert at this location, although the absolute displacement in itself is lower (Fig. 2c). Impacting the beam in the Y-direction that refers to a larger second moment of area and hence a higher stiffness translated into much lower damping, which corroborated this further. This collectively presented the first indication of frictional energy dissipation from interfacial microslip being a mechanism of damping, and the potential role of an EDM texture in influencing it.

Encouraged by the considerable increase in damping obtained for the EDM texture that referred to discharge parameters chosen arbitrarily for the preliminary experiment (Fig. 2b), further effort was expended on systematically characterising the damping performance of textures generated over an expansive range of  $i_e$  and  $t_e$ . Results shown in Fig. 2d indicate  $\zeta$  to exhibit defined maxima at distinct discharge durations depending on the discharge current, with the optimal duration shifting to lower values with an increase in current. Overall, a maximum  $\zeta$  of over 3% could be achieved, which represents a 100% enhancement relative to the extruded control treatment.

In the interest of texturing speed, further experiments employed  $i_e$  of 72 A and the corresponding optimal  $t_e$  of 65  $\mu\text{s}$ . Higher  $i_e$  could not be tried due to the limitation of the machine tool power generator; inserts of  $85 \times 20 \text{ mm}^2$  area used in this work could however be textured within several seconds using this set of discharge parameters. The damping performance of textures generated using this combination was further tested to be robust to repositioning of the damping insert, changes in clamping torque, and between insert samples.

To comprehend the role of the discharge parameters in physical terms, the topography of a representative set of surfaces spanning the range of  $\zeta$  obtained was characterised. Perhaps unsurprisingly,  $\zeta$  was found uncorrelated with the  $Ra$  roughness (Fig. 3a). It may be noted that  $\zeta$  was presented only in terms of the  $Ra$  parameter in [7], but the number of surfaces investigated therein was limited to just three, which as well corresponded to a change in only  $i_e$ , as mentioned previously.  $\zeta$  did however correlate well with the surface skewness  $Rsk$  and kurtosis  $Rku$  parameters, with the fit surface seen in Fig. 3b capturing 80% of the variation in the data. A positive skewness points to a predominance of peaks over valleys in the surface profile. A kurtosis value

over 3 indicates these peaks to be higher relative to those that conform to a normal distribution. The inset in Fig. 3b provides a qualitative representation of such a profile from [5]. A significant interaction between the  $Rsk$  and  $Rku$  parameters is also evident, quite in alignment with the theoretical prediction (Fig. 1a) of Medina et al. [5]. This underscores the unique capability of EDM textures for vibration control as posited in Section 1 of this paper. Such validation is significant also in the design and development of deterministic surfaces for vibration damping applications, which may be realised using additive manufacturing technologies.

With a view to decoding the mechanism of damping associated with EDM-textured interfaces, surfaces referring to three  $t_e$  for a constant  $i_e$  of 72 A were chosen with intent for examination in a confocal microscope. Figure 3c is a

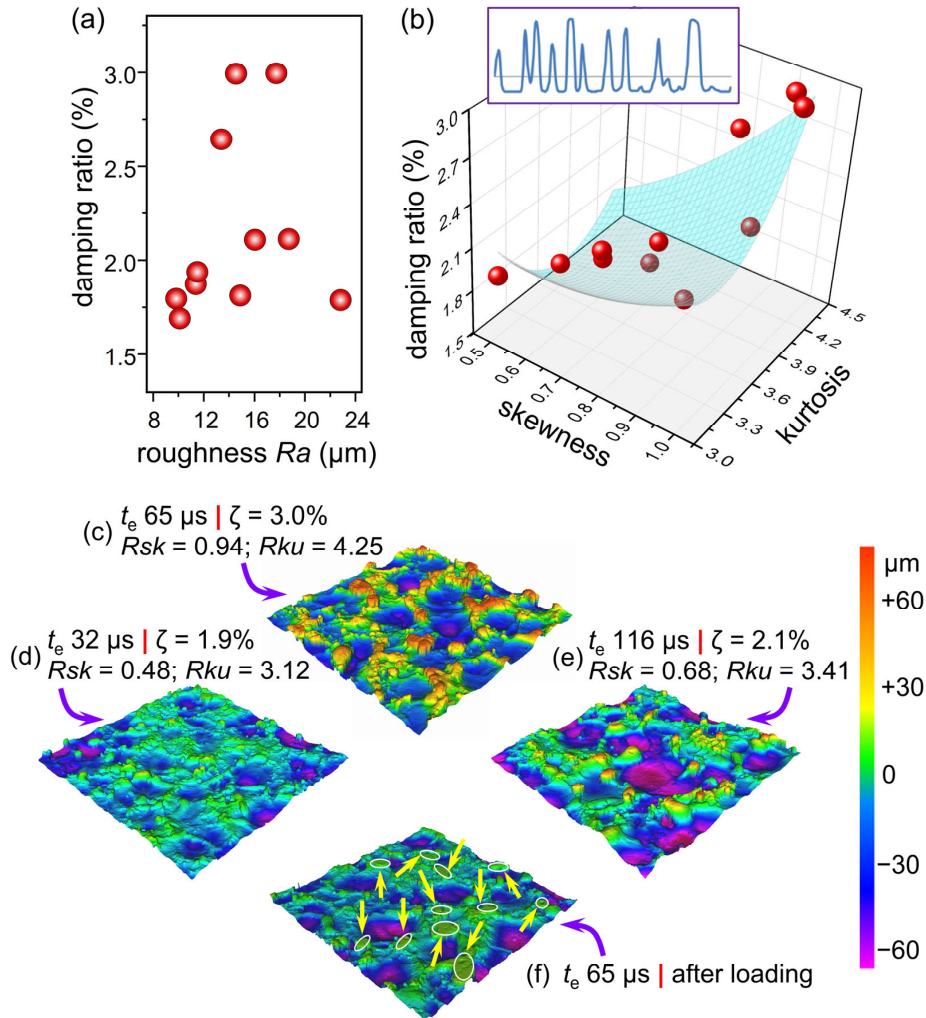


Fig. 3. Effect of: (a)  $Ra$  roughness, and (b) skewness and kurtosis, on damping ratio; (c–f): confocal micrographs of textured surfaces ( $1.6 \times 1.6 \text{ mm}^2$ ).

micrograph of the surface corresponding to  $t_e$  of  $65 \mu\text{s}$  that yielded the maximum  $\zeta$  of 3%; juxtaposed to this are Figs. 3d and 3e, which relate to surfaces immediately adjacent to and on either side of the maximum returning lower  $\zeta$  of 1.9% and 2.1% at  $t_e$  of  $32 \mu\text{s}$  and  $116 \mu\text{s}$ , respectively (see Fig. 2d). The best performing texture (Fig. 3c) is readily differentiated by the conspicuous presence of a number of surface protrusions of height  $\sim 50 \mu\text{m}$ .

Perusal of Fig. 3c further reveals these protrusions to be populated around the rims of individual craters (that map to the blue and purple domains of the colour scale). This points to their being resolidified material that was expelled from and strewn around the molten crater on implosion of the gas bubble towards the end of the discharge pulse, resembling ejecta found around meteoritic craters. Such features are entirely absent in Fig. 3d, and are highly limited in terms of their prevalence and magnitude in Fig. 3e, in direct correlation to the  $Rsk$  and  $Rku$  parameters, and the damping ratios shown alongside these surfaces in the figure. Although they are an impediment to material removal and surface quality in common EDM applications, resolidified material in the form of isolated protrusions is incidentally advantageous insofar as vibration damping is concerned. Figure 3f represents a surface similar to that in Fig. 3c but after loading, wherein the regions highlighted by the arrows show the protrusions to have been squished down. It follows therefore that these protrusions anchor themselves against the counterface and dissipate energy in response to the imposed normal and tangential forces, similar to what transpires in fretting contacts [9].

Microslip is an intriguing feature of Hertzian contacts subject to tangential loading. For a spherical asperity loaded with a normal force against a flat counterface, the frictional stress increases axisymmetrically from zero at the contact perimeter to a maximum at the centre, following the normal stress distribution (Fig. 4a). Simultaneous application of a tangential load induces a shear stress that is also axisymmetric, which does but increase from a finite minimum at the centre to an infinite value at the outer edge. It is not commonly appreciated therefore that for all tangential loads—not limited to any minimum threshold—a peripheral microslip region is manifested in the annulus where the shear stress exceeds the limiting frictional stress (Fig. 4a), as clarified by the Cattaneo-Mindlin model [9]. With increasing tangential load, the slip annulus grows radially inward at the expense of the stick region, until the contact eventually suffers complete slip. Much as this model is insightful, experiments have shown it to underpredict the energy dissipation prior to incipient gross slip. This has since been reconciled [10] by recognising the elasto-plastic nature of the contact zone and acknowledging a plastic annulus

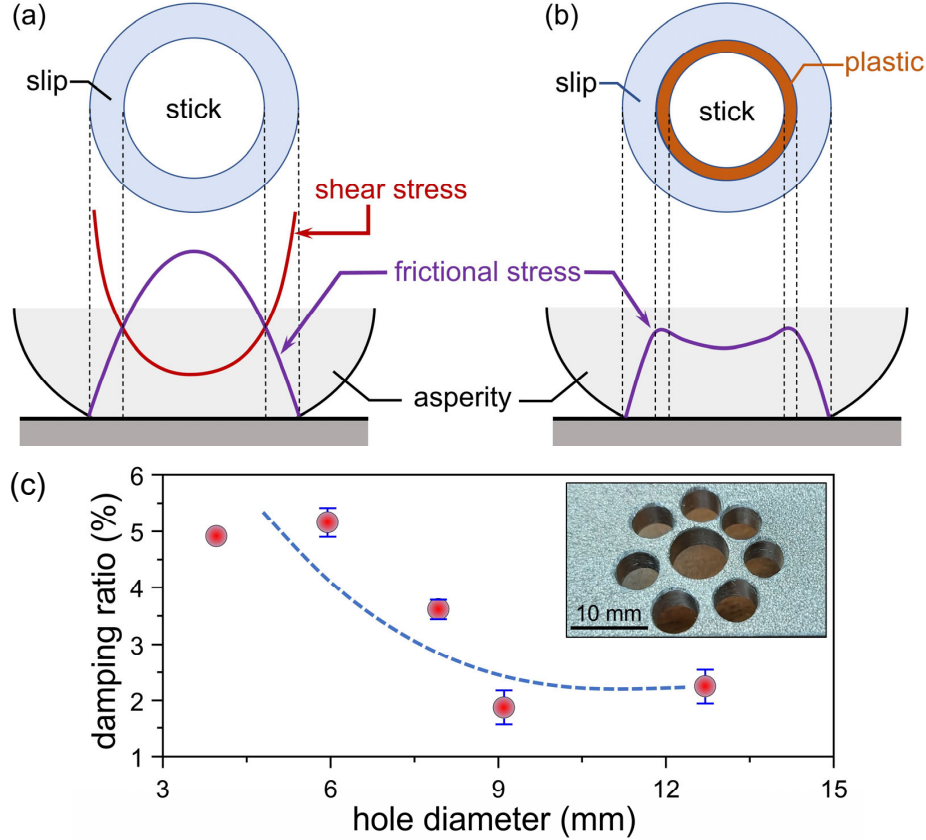


Fig. 4. (a,b) Mechanism of energy dissipation; after [10]; (c) effect of hole diameter on damping performance.

between the stick and slip annuli (Fig. 4b). Reciprocating tangential loads will therefore dissipate energy through repeated microslip and plastic deformation at the protruding asperities (as those seen in Fig. 3c).

Following the insight that energy dissipation tends to materialise in the vicinity of edges where the frictional stress approaches zero (Fig. 4a), it was deemed that the damping capacity of textured inserts could be further enhanced through the introduction of additional edges by drilling holes around the bolt hole (see inset in Fig. 4c) where the relatively higher clamping pressure tends to restrain microslip. Such an approach has been investigated by Wentzel et al. in [11]. To verify this hypothesis, textured inserts with holes of different diameters were evaluated using the experimental set-up shown in Fig. 2a. To ensure parity, the number of holes for each diameter was determined such that the total area lost to holes was held constant at  $\sim 23\%$ . The data shown in Fig. 4c proves the premise above and indicates that  $\zeta$  could be increased to over 5%, which is more than a five-fold enhancement relative to the baseline with no inserts (Fig. 2b). Hole edges were further found to be selectively

burnished smooth, implying localised plastic deformation as noted in Fig. 4b.

### 3.2 Application

The second phase of this research examined the efficacy of enhancing the stability of a grooving process through the strategic placement of EDM-textured damping inserts in the grooving blade holder assembly. Tests involved a steel blade of section  $31.9 \times 3.7 \text{ mm}^2$  and overhang 50 mm, which was held against and into a blade holder (Fig. 5a) using a top mount with three M6 screws torqued to 11 Nm; this assembly was in turn secured in a turret station using two M8 bolts subject to the same torque.

The performance of the following three cases was compared: (1) commercial tool assembly used as is to constitute the baseline, (2) tool assembly with untextured extruded aluminum inserts, and (3) tool assembly with aluminum

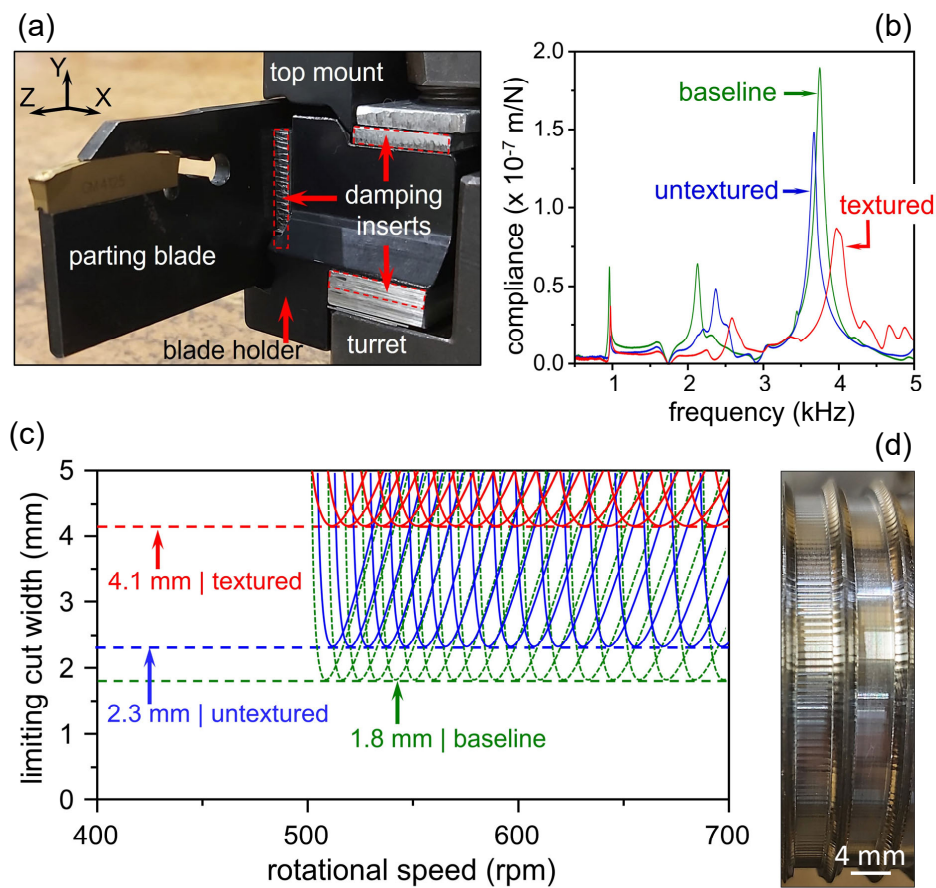


Fig. 5. (a) Grooving tool assembly, (b) its cross FRF, (c) stability lobe diagram, and (d) experimental verification.

damping inserts textured with the best discharge parameters ( $i_e$  72 A,  $t_e$  65  $\mu$ s) and comprising 4 mm diameter holes. A finite element analysis revealed a torsional mode and two bending modes of vibration, and offered the insight that the vertical interface between the blade and the blade holder (YZ-plane) and the two horizontal interfaces between the blade holder and the turret station (XZ-plane) to be the best suited to sandwich the damping inserts into (Fig. 5a).

Tap tests were conducted to assess the three cases above as per Saffury [12] who identified the cross FRF between the cutting (Y) and feed (Z) directions to characterise the stability of grooving tools. The corresponding data revealed the textured insert to refer to a higher dynamic stiffness, for the critical third mode in particular (Fig. 5b). Pertinent modal information was extracted from the FRFs to compute the stability lobes as outlined in [12], for AISI 4340 steel. This predicted the textured insert to increase the absolute stability limit to 4.1 mm, which is a  $\sim$ 200% enhancement relative to the baseline (Fig. 5c). This was verified experimentally by machining grooves with a 4 mm straight edge tool at a speed of 165 m/min and an infeed of 0.2 mm/rev. The machined groove on the left in Fig. 5d that exhibits the distinctive chatter signature is representative of the baseline and untextured cases, both of which developed instability. In contrast, the textured damping insert related to stable machining as denoted by the smooth groove on the right in Fig. 5d, validating the prediction in Fig. 5c and proving the concept of EDM-textures for vibration control. The performance of the damping insert was further found to be unaffected by the application of a cutting fluid.

## 4 Conclusions

This research advanced the novel, unconventional application of EDM-textured damping inserts for passive vibration damping. An investigation of the effect of discharge parameters showed that the damping ratio could be doubled relative to an extruded insert. Damping performance was found to correlate with the combined increase of positive skewness and high kurtosis of surface height that are unique characteristics of EDM surfaces. The damping mechanism was identified to be microslip and plastic deformation around the edges of protruding asperity contacts. This prompted the idea of drilling holes in the textured insert so as to tap into the additional edges, which further enhanced damping. The knowledge generated in this work was applied to increase the stability-limited cut width of a grooving tool by a factor of over 2. This high-

lights the far-reaching potential of this innovative technology in the broader realm of vibration control.

## References

- [1] Munoa J, Beudaert X, Dombovari Z, Altintas Y, Budak E, Brecher C, Stepan G (2016) Chatter Suppression Techniques in Metal Cutting. *CIRP Annals—Manufacturing Technology* 65(2):785–808.
- [2] Ziegert JC, Stanislaus C, Schmitz TL, Sterling R (2006) Enhanced Damping in Long Slender End Mills. *Journal of Manufacturing Processes* 8(1):39–46.
- [3] Hayati S, Shahrokhi M, Hedayati A (2021) Development of a Frictionally Damped Boring Bar for Chatter Suppression in Boring Process. *International Journal of Advanced Manufacturing Technology* 113:2761–2778.
- [4] Ito Y, Masuko M (1975) Study on the Damping Capacity of Bolted Joints: Effects of Joint Surface Conditions. *Bulletin of Japanese Society of Mechanical Engineers* 18(177):319–326.
- [5] Medina S, Olver AV, Dini D (2012) The Influence of Surface Topography on Energy Dissipation and Compliance in Tangentially Loaded Elastic Contacts. *Journal of Tribology* 134(1):011401.
- [6] Whitehouse DJ, *Handbook of Surface and Nanometrology*, CRC Press, Boca Raton, 2011.
- [7] Beards CF, Neroutsopoulos AA (1980) The Control of Structural Vibration by Frictional Damping in Electro-Discharge Machined Joints. *Journal of Mechanical Design* 102(1):54–57.
- [8] Rogers PF, Boothroyd G (1975) Damping at Metallic Interfaces Subjected to Oscillating Tangential Loads. *Journal of Engineering for Industry* 97(3):1087–1093.
- [9] Stachowiak GW, Batchelor AW, *Engineering Tribology*, Elsevier Butterworth-Heinemann, Oxford, 2005.
- [10] Ödfalk M, Vingsbo O (1992) An Elastic-Plastic Model for Fretting Contact. *Wear* 157(2):435–444.
- [11] Wentzel H, Olsson M, Oberg M (2008) Metallic Inserts as a Tool to Alter the Structural Damping of Joined Structures. *International Journal of Surface Science and Engineering* 2(1):152–167.
- [12] Saffury J (2017) Chatter Suppression of External Grooving Tools. *Procedia CIRP* 58:216–221.